

Frequency measurement of the $6P_{3/2} \rightarrow 7S_{1/2}$ transition of thallium

Nang-Chian Shie,¹ Chun-Yu Chang,² Wen-Feng Hsieh,¹ Yi-Wei Liu,^{3,4} and Jow-Tsong Shy^{2,3,4,*}

¹*Department of Photonics and Institute of Electro-Optical Engineering, National Chiao Tung University, 30050 Hsinchu, Taiwan*

²*Institute of Photonics Technologies, National Tsing Hua University, 30013 Hsinchu, Taiwan*

³*Department of Physics, National Tsing Hua University, 30013 Hsinchu, Taiwan*

⁴*Frontier Research Center on Fundamental and Applied Sciences of Matters, National Tsing Hua University, Hsinchu 30013, Taiwan*

(Received 9 October 2013; published 30 December 2013)

The saturated absorption spectrum of the $6P_{3/2} \rightarrow 7S_{1/2}$ transition of ^{203}Tl and ^{205}Tl in a hollow cathode lamp has been observed with a frequency-doubled 1070 nm Nd : GdVO₄ laser. The third-derivative spectrum of the hyperfine components are obtained using the wavelength modulation spectroscopy and used to stabilize the laser frequency. The analysis of the error signal shows that the frequency stability reaches 30 kHz at 1 s averaging time. Such a frequency-stabilized light source at 535 nm can be used for laser cooling of thallium and for investigating the parity non-conservation effect in thallium. The absolute frequencies of hyperfine components are measured with an accuracy of 30 MHz using a precision wavelength meter. Including the pressure shift correction, the center of gravity of the transition frequency is determined to an accuracy of 22 MHz for both isotopes. Meanwhile, the isotope shift derived is in good agreement with earlier measurement.

DOI: [10.1103/PhysRevA.88.062513](https://doi.org/10.1103/PhysRevA.88.062513)

PACS number(s): 32.10.Fn, 32.30.-r

I. INTRODUCTION

High precision measurements of the parity non-conservation (PNC) effects and the permanent electric dipole moment (EDM) using atomic systems are promising in testing the standard model (SM) and searching for new physics. Heavy atoms, such as cesium (Cs) and thallium (Tl), are adopted in the PNC and EDM experiments because these symmetry violation effects are enhanced by their large atomic number. However, in the atomic PNC measurement, an accurate theoretical calculation of atomic structure is needed for such test. In the case of Cs, a PNC measurement of 0.35% accuracy combined with a calculation of 0.5% accuracy leads to the most accurate result for the weak charge of cesium nucleus, which can be compared with the prediction of the SM [1,2]. On the contrary, the 1.7% uncertainty of the PNC experiment in the Tl system using the $6P_{1/2} \rightarrow 6P_{3/2}$ transition [3,4], combining with the 2.5% accuracy of Tl atomic theory, leads to a total uncertainty of 3.0% for the weak charge of thallium nucleus. The Tl atom, which has only one unpaired electron, is one of the best candidates to measure the weak charge of nucleus. However, its atomic structure is more complicated than the alkali metals and the accuracy of theoretical calculation is limited. Precision measurements of thallium atomic structure, such as the absolute transition energy, hyperfine splitting (HFS) and isotope shift can serve as the experimental constraints and benchmarks for the improvements of theory.

On the other hand, the measurement of the electric dipole moment of atomic Tl [5] has been the most precise experiment to set the upper limit of electron's EDM for decades, until the recent improvement using molecular YbF [6]. The implementation of laser cooling on atomic thallium, which produces slow intense atomic beam or ultracold sample, can offer great advantages for further reducing systematic uncertainties and increasing signal strength for the EDM experiment. A cooling

scheme based on the metastable $6P_{3/2}$ state has been proposed and investigated [7]. It utilizes the $6P_{1/2} \leftrightarrow 6D_{5/2}$ transition, which has a high transition rate and can be considered as a nearly closed two-level cooling cycle. However, the difficulty of this scheme is the availability of high power 352 nm cooling UV laser source. An alternative approach is the two-color Λ type cooling scheme, which can be adapted to group III atoms and has been realized for cooling indium [8]. In atomic thallium, as the energy levels show in Fig. 1, it involves the $6P_{1/2} - 7S_{1/2} - 6P_{3/2}$ transitions at 378 nm and 535 nm. Therefore, stable and powerful laser sources are required to access these transitions and to achieve such a cooling scheme. Especially, a single frequency tunable 535 nm laser was only available with a dye laser system before 2011 [9]. In addition, a stabilized 535 nm laser can be applied to the electromagnetically induced transparency (EIT) measurement which may improve the sensitivity of the PNC measurement [10].

The simplified low-lying energy levels of thallium are shown in Fig. 1 with the most precise values of HFS and isotope shifts. Early literatures have reported precise HFS measurements with uncertainties <1 kHz for both $6P_{1/2}$ and $6P_{3/2}$ states using microwave magnetic resonance techniques in the 1950s [11,12]. Recently precise measurements of the absolute transition frequency and the HFS of the $6P_{1/2} \rightarrow 7S_{1/2}$ transition have been reported [13]. However, no precise measurements have been carried out for the $6P_{3/2} \rightarrow 7S_{1/2}$ transition at 535 nm up to now.

In this paper, we report a precise measurement of the absolute frequencies of hyperfine components of the 535 nm $6P_{3/2} \rightarrow 7S_{1/2}$ transition for ^{203}Tl and ^{205}Tl using an all-solid-state laser system [9]. A hollow cathode lamp (HCL) is utilized to provide vapor of the atomic thallium at the metastable $6P_{3/2}$ state. The saturation spectroscopy is employed to resolve all the hyperfine transitions, and their absolute frequencies are measured using a precision wavelength meter. We have achieved the frequency determination of the center gravity of the $6P_{3/2} \rightarrow 7S_{1/2}$ transition with accuracy better than 22 MHz for both isotopes.

*shy@phys.nthu.edu.tw

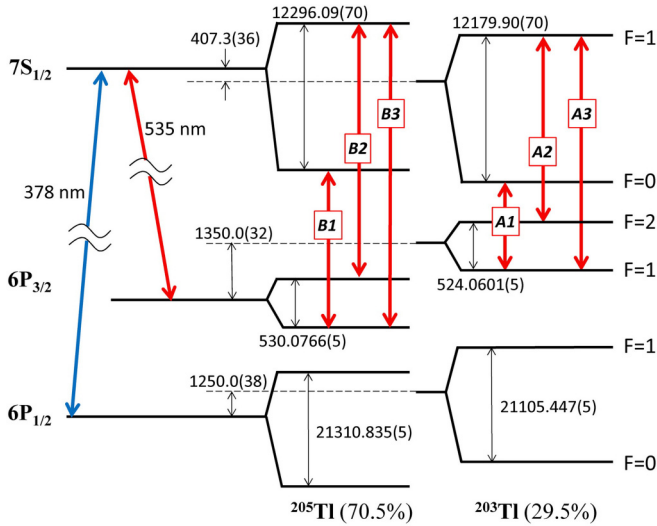


FIG. 1. (Color online) Energy-level diagram of ^{203}Tl and ^{205}Tl with the hyperfine splittings and isotope level shifts in the unit of MHz. Energy levels are not to scale. The six lines investigated in this work are labeled A1, A2, A3 and B1, B2, B3. The hyperfine splittings of $6P_{3/2}$ and $6P_{1/2}$ are taken from [11] and [12], respectively. The hyperfine splittings of $7S_{1/2}$ are taken from [13]. The level isotope shifts are taken from [14].

II. EXPERIMENT

The scheme of our experimental setup for the absolute frequency measurements of the hyperfine components of the $535\text{ nm } 6P_{3/2} \rightarrow 7S_{1/2}$ transition of Tl is shown in Fig. 2. The laser source is a frequency-doubled 1070-nm Nd:GdVO₄ laser. The laser uses a volume Bragg grating (VBG) as the output coupler and wavelength selector. This 1070-nm laser is similar to our previous design [9] except an Nd:GdVO₄ laser crystal

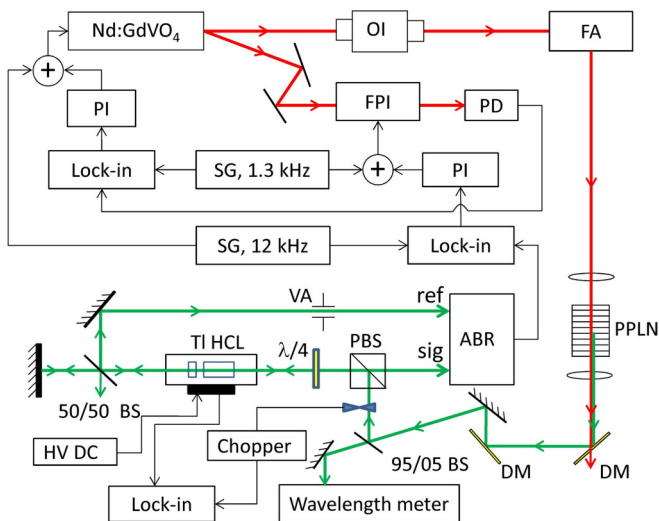


FIG. 2. (Color online) The experimental setup. OI: optical isolator, FA: fiber amplifier, FPI: Fabry-Perot interferometer, PD: photodiode, PI: PI servo loop, SG: signal generator, Lock-in: Lock-in amplifier, VA: variable aperture, ABR: auto-balanced receiver, BS: beam splitter, $\lambda/4$: quarter-wave plate, DM: dichroic mirror, HV DC: high voltage dc power supply for HCL.

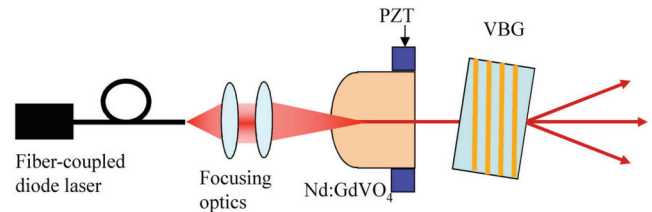


FIG. 3. (Color online) Schematic diagram of the single frequency Nd:GdVO₄ laser. VBG: volume Bragg grating; PZT: piezoelectric transducer.

with a spherical input surface ($R = 30\text{ cm}$, HT at 808 nm, HR at 1070 nm) and a flat end surface (AR at 808 and 1070 nm) is adopted to improve the mechanical stability, as shown in Fig. 3. The spherical surface of this laser crystal acts as the concave mirror of the plano-concave laser cavity. The laser crystal is mounted on a piezoelectric transducer (PZT) for cavity length tuning. There are three main output beams with almost same power due to the reflections of the Bragg grating planes and the VBG surfaces. All outputs are linearly polarized. The central laser beam is used to carry out the spectroscopic experiment. To reduce the environmental disturbances, the entire laser assembly is put in an aluminum housing whose temperature is stabilized by a thermoelectric cooler. The frequency of the laser can be tuned coarsely by the VBG temperature and finely by the PZT voltage. To reduce the laser frequency drift it is locked to a confocal Fabry-Perot interferometer (FPI). One of the other output beams is directed into the confocal FPI and the FPI cavity length is modulated at 1.3 kHz. The 1070 nm light signal after the FPI cavity is demodulated to obtain the error signal for locking the laser frequency to the FPI. The laser frequency is then tuned by scanning the FPI cavity length after it is locked. In our experiment, the VBG is heated to $\sim 42.5^\circ\text{C}$ to generate the correct wavelength for the $6P_{3/2} \rightarrow 7S_{1/2}$ transition after frequency doubling. By tuning the PZT, the single frequency tuning range without mode-hopping at total output power $> 100\text{ mW}$ is about 5 GHz at 1070 nm, which is not wide enough to cover the whole $6P_{3/2} \rightarrow 7S_{1/2}$ hyperfine transitions after frequency doubling. Therefore, the whole spectrum of the $6P_{3/2} \rightarrow 7S_{1/2}$ transition is divided into two regions to be separately investigated and the center of each region is set by tuning the VBG temperature.

The central beam of the VBG laser is boosted by a 900-mW Yb-doped fiber amplifier. The amplified 1070 nm laser beam is then focused into a 50 mm long MgO-doped periodically poled lithium niobate (MgO:PPLN) crystal with a lens ($f = 100\text{ mm}$) for frequency doubling. The PPLN crystal is mounted in a temperature-stabilized oven and the quasi-phase matching condition is achieved around 101°C . After passing through the PPLN, the 1070 nm beam is separated out by two dichroic mirrors (DMs) and the second harmonic 535 nm green beam is collimated to a beam size of 8.4 mm in diameter. The power of 535 nm beam after these two DMs is typically 46 mW with 700 mW 1070 nm fundamental pump power.

A commercially available see-through hollow cathode lamp (HCL) is used as the thallium atomic source. HCL is a metal-vapor discharge lamp specifically developed for atomic absorption spectroscopy and narrow band atomic line filter

[15]. Exciting the HCL with a high voltage source, a discharge plasma is generated inside the cathode. HCL produces not only sufficient metal vapor without high temperature oven, but also the atoms at the excited states. When a laser enters the cathode and the atoms inside the discharge plasma resonantly interact with the incident photons, the electrical impedance of the discharge plasma is altered, by which an optogalvanic (OG) signal is obtained. Optogalvanic effect has been widely used to stabilize laser frequency [16]. In our experiment, a Hamamatsu L2783-81 NE-TL see-through HCL is used as the thallium vapor cell. The cylindrical cathode (19 mm in length and 3 mm in diameter) and the ring anode are sealed with neon buffer gas at a pressure of 14 torr. The HCL is operated at a current of 10.7 mA with a 30 k Ω ballast resistor.

The absorption lines of thallium in the HCL are Doppler-broadened by the random thermal motion of the thallium atoms. Saturated absorption spectroscopy is used to eliminate the Doppler-broadening by counter-propagating a strong pump beam over the probe beam. The linear polarized green light passes through a 95:5 (R:T) beam splitter (BS) reaches a precision wavelength meter (HighFinesse, WSU 30) for frequency measurement. The beam reflected by the BS is further reflected by a polarizing beam splitter (PBS) and transformed into circular polarization by a quarter-wave plate ($\lambda/4$), and then goes through the HCL acting as the pump beam. The circularly polarized green light is further separated by a 50/50 beam splitter. The beam passing through the BS is retro-reflected by a mirror into the HCL acting as the probe beam. The reflected light is then transformed into linear polarization by going through the $\lambda/4$ plate again and passes through the PBS to the signal input of an auto-balanced receiver (ABR, New Focus, 2017 Nirvana). The auto-balanced receiver is used to suppress the intensity noise of the 535 nm light. The counter-propagated pump and probe beams are overlapped within the HCL with powers of 12.5 mW and 2.7 mW, respectively. The beam reflected by the 50/50 BS is directed into the reference input of the auto-balanced receiver. The optimal power ratio of the signal to the reference beam for noise cancellation is achieved by a variable aperture in front of the reference input.

To tune the laser wavelength to the thallium transition, the 535 nm green light is first amplitude modulated by a mechanical chopper at 2 kHz. The optogalvanic signal from the HCL is detected with a lock-in amplifier (Standard Research Systems SR830) to obtain the Doppler broadened spectrum of the $6P_{3/2} \rightarrow 7S_{1/2}$ transition by tuning the laser frequency via scanning the FPI cavity length. To obtain the third-derivative saturated absorption spectrum of the hyperfine transition, the laser cavity length is modulated at 12 kHz and the balanced signal from the auto-balanced receiver is demodulated with a lock-in amplifier at the third harmonics (36 kHz). The time constant is set to 30 ms at 12dB/oct. To lock the laser frequency to the center of the hyperfine transition, the demodulated signal is feed through a PI (proportional and integral) servo loop to control the FPI cavity length.

The absolute transition frequencies are measured using the precision wavelength meter. It is a Fizeau based wavelength meter and a similar wavelength meter has been used to measure the hyperfine splitting in Cs to an accuracy of 0.5 MHz [17,18]. Our wavelength meter has an absolute accuracy of 30 MHz in

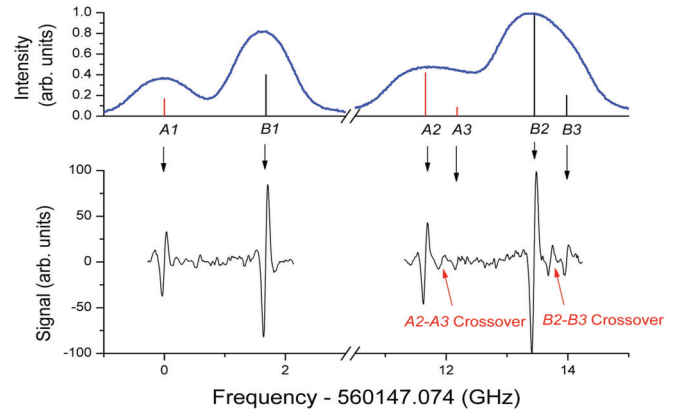


FIG. 4. (Color online) Observed spectrum of hyperfine components of the $6P_{3/2} \rightarrow 7S_{1/2}$ transition in atomic thallium at 535 nm. The upper figure is the optogalvanic (OG) spectrum. Vertical lines show the calculated spectral intensity. The lower figure is the third-derivative signal of the saturated absorption spectrum.

10 h [19] after it is calibrated against a stabilized laser with an accurately known frequency. In our work, a frequency doubled Nd:YAG laser at 532 nm stabilized to the hyperfine component a_{10} of $R(56)$ 32-0 transition of molecular iodine is utilized to calibrate the wavelength meter. Its absolute frequency has been recommended as an optical frequency standard [20,21]. We find that the drift of the wavelength meter is less than 1 MHz within 10 min after calibration. To check the accuracy of the wavelength meter at 535 nm, the frequency doubled Nd:GdVO₄ laser is stabilized to the hyperfine components of the $P(28)$ 30-0 transition of molecular iodine at 535 nm, which is less than 10 GHz away from the thallium transitions. The absolute frequencies of the a_1 , a_{10} , and a_{15} hyperfine components have been measured using an optical frequency comb (OFC) to an accuracy of 11 kHz [22]. The differences between the absolute frequencies measured by the wavelength meter and the OFC are less than 3 MHz for all three hyperfine components. In addition, the separation of hyperfine components obtained by the wavelength meter is less than 1 MHz deviation from the values obtained by OFC. To avoid the long time drift in the wavelength meter during frequency measurement, the calibration using iodine-stabilized 532 nm laser is carried out every 10 min to assure the accuracy of our measurements is better than 30 MHz.

III. RESULTS AND DISCUSSION

The $6P_{3/2} \rightarrow 7S_{1/2}$ transition for ^{203}Tl and ^{205}Tl consists of six hyperfine components as shown in Fig. 1. These hyperfine components are labeled as A1, A2, A3 and B1, B2, B3 for ^{203}Tl and ^{205}Tl , respectively. The output of the lock-in detection of the discharge current modulation, due to the laser intensity modulation by the mechanical chopper, provides the OG spectrum shown in the upper curve of Fig. 4. The hyperfine components of $6P_{3/2} \rightarrow 7S_{1/2}$ transition are not resolved in the OG spectrum due to the Doppler broadening. The Doppler-free saturated absorption spectrum is shown in the lower part of Fig. 4. For the strongest component B2, the signal-to-noise ratio (SNR) is 220. The ratio of the signal

strength between the observed transitions does not agree with the predicted strength based on the transition rate calculation (shown in the OG spectrum in Fig. 4). This discrepancy, which was also observed in the emission profile of the earlier literature [15], is attributed to the high drive current of the HCL. The SNR of the A1, A2, B1, and B2 components is high enough for laser frequency stabilization and direct frequency measurement using the HighFinesse wavelength meter.

The observed saturated absorption spectrum shown in Fig. 4 is acquired using a frequency modulation width that is optimized for the third-derivative signal of the B2 component. For a spectral line with a Lorentzian profile, the third derivative signal reaches a maximum while the modulation width is $1.75 \times \text{FWHM}$ (full width at half-maximum) and the peak-to-peak frequency interval then equals to $1.65 \times \text{FWHM}$ [23]. The peak-to-peak frequency interval is 70 MHz in our experiment, thus the FWHM of the B2 component is 42 MHz. For comparison, the natural linewidth of the B2 component is estimated to be 17 MHz by the lifetime of $7S_{1/2}$ state [24].

The absolute frequency measurements of the $6P_{3/2} \rightarrow 7S_{1/2}$ hyperfine transitions are performed using the HighFinesse wavelength meter, while the laser is locked to the zero-crossing points of the third derivative signal. The error signal of the stabilized laser is used to evaluate the stability of the laser frequency. The 70 MHz peak-to-peak frequency interval of the third-derivative signal of the B2 component is employed to determine the frequency discrimination slope. Figure 5 shows the Allan deviation for the frequency doubled Nd:GdVO₄ laser stabilized at the B2 component. The frequency stability is 30 kHz at 1 s averaging time and reaches 2 kHz at 10 s. This frequency stabilized laser system is suitable for the thallium laser cooling experiment and for investigating the PNC effect in thallium using the EIT technique in the future.

Each measurement of the locked laser frequency is completed in 5 minutes after calibration of the wavelength meter. The accuracy of the wavelength meter is rechecked with the calibration laser after every measurement. The laser is unlocked and relocked between each measurement. More than

5000 data are taken for an individual measurement and more than 20 frequency measurements are taken for each transitions. The standard deviations for each frequency measurement of these four strong components is from 0.8 to 2.6 MHz, depending on the SNR. The standard errors of the mean, as the statistical uncertainty of the central frequency for these hyperfine transitions, are from 8 to 18 kHz. Various systematic uncertainties are also studied, including: 0.6 MHz error due to the DC-offset of the third derivative signal and 0.2 MHz uncertainty caused by the electronic noise. However, the final accuracies of frequency measurements, which are dominated by the accuracy of the wavelength meter, are 30 MHz for all of the A1, A2, B1, and B2 components.

The signal amplitude of A3 and B3 components are too small to stabilize the laser for a direct frequency measurement. Alternatively, the frequency intervals A2-A3 and B2-B3 are acquired from the observed spectrum by scanning the laser frequency. The third derivative spectrum in Fig. 4, where the frequency axis is given by simultaneously acquiring the wavelength meter output, is obtained in a total measuring time of 10 min. Two crossover signals of A2, A3 and B2, B3 components can be also observed in the spectrum. In this method, two major systematic errors must be taken care: the DC-offset of the signal and the determination of the zero-crossing point (the line center). The DC-offset of the third derivative signal is carefully removed before performing the frequency interval measurement. The zero-crossing point frequencies are determined using the cubic spline interpolation of the nearby data points. Data analysis for 12 upward and downward laser frequency scans gives the frequency intervals of 524.6(1.1) MHz and 531.64(50) MHz for A2-A3 and B2-B3 components, respectively. Our results agree very well with the best previous measurements [12]. With the measured absolute frequencies of A2 and B2 components, the absolute frequencies of A3 and B3 component are then derived from the A2-A3 and B2-B3 frequency intervals. Combining with the precise values of HFSs of $6P_{3/2}$ [12] and $7S_{1/2}$ [13], we are able to derive the center of gravity (c.g.) of the $6P_{3/2} \rightarrow 7S_{1/2}$ transition frequency with an accuracy of 17 MHz. The results of the absolute frequency measurements of the hyperfine components of ^{203}Tl and ^{205}Tl at 14 torr Ne background pressure are listed in Table I. The isotope shift

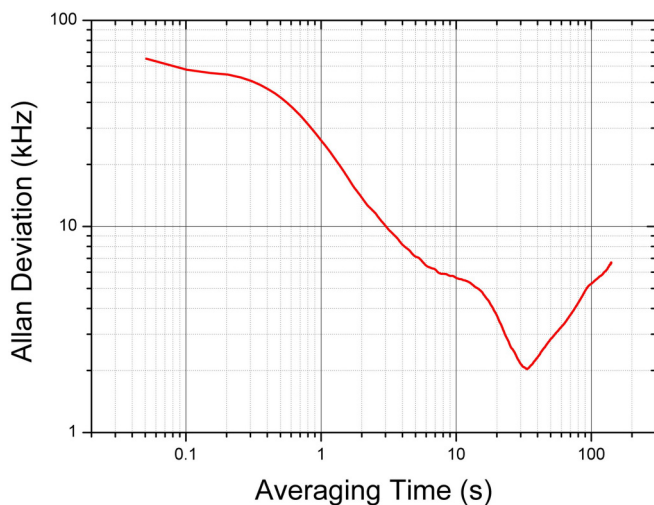


FIG. 5. (Color online) Allan deviation of the laser locked to B2 component at 535 nm.

TABLE I. The absolute frequencies of the hyperfine components within $6P_{3/2} \rightarrow 7S_{1/2}$ transition of ^{203}Tl and ^{205}Tl in HCL at a background neon pressure of 14 torr.

Line	$F - F'$	Frequency (MHz)
A1	$^{203}\text{Tl}, 1 - 0$	560 147 075(30)
B1	$^{205}\text{Tl}, 1 - 0$	560 148 751(30)
A2	$^{203}\text{Tl}, 2 - 1$	560 158 729(30)
A3	$^{205}\text{Tl}, 1 - 1$	560 159 254(30)
B2	$^{203}\text{Tl}, 2 - 0$	560 160 514(30)
B3	$^{205}\text{Tl}, 1 - 1$	560 161 045(30)
c.g. of ^{203}Tl	$6P_{3/2} \rightarrow 7S_{1/2}$	560 155 881(17)
c.g. of ^{205}Tl	$6P_{3/2} \rightarrow 7S_{1/2}$	560 157 638(17)
Experiment(^{205}Tl) [24]	$6P_{3/2} \rightarrow 7S_{1/2}$	560 156.2 (GHz)
Theory(^{205}Tl) [25]	$6P_{3/2} \rightarrow 7S_{1/2}$	558 183.6 (GHz)

(IS) of this transition is calculated to be 1757(24) MHz, which is consistent with the previous result [14], by subtracting the c.g. frequencies of the two isotopes.

The pressure shift of this transition under neon has been measured to be $-2.3(1.0)$ MHz/torr [26]. Therefore, by taking the pressure shift (-33 ± 14 MHz) into account, the zero-pressure transition frequencies of the $6P_{3/2} \rightarrow 7S_{1/2}$ transition is determined to be 560 155 914(22) MHz and 560 157 671(22) MHz for ^{203}Tl and ^{205}Tl , respectively. The energy of the $6P_{3/2} \rightarrow 7S_{1/2}$ transition has been calculated to be 18619 cm^{-1} , corresponding to 558 183.6 GHz, using the many-body perturbation theory (MBPT) with the configuration interaction (CI) method [25].

IV. CONCLUSIONS

In summary, the saturated absorption spectrum of the hyperfine components of the $6P_{3/2} \rightarrow 7S_{1/2}$ transition of ^{203}Tl and ^{205}Tl in a hollow cathode lamp has been observed using a tunable frequency doubled 1070 nm Nd:GdVO₄ laser. The

laser can be frequency stabilized to the four strong hyperfine components with a stability of 30 kHz at 1 s averaging time. This compact 535 nm laser system has a power >50 mW and a frequency tuning range of 10 GHz. It will be used for the thallium laser cooling experiment and for the PNC measurement in thallium using EIT in the future. Furthermore, the absolute frequencies of the hyperfine components have been measured using a precision wavelength meter with accuracy of 30 MHz. Combining with previous accurate HFS of the $6P_{3/2}$ and $7S_{1/2}$, the c.g. of the transition frequency of $6P_{3/2} \rightarrow 7S_{1/2}$ is determined to an accuracy of 22 MHz (better than 4×10^{-8}) for both isotopes. Finally, the isotope shift of $6P_{3/2} \rightarrow 7S_{1/2}$ transition determined is also in good agreement with the previous measurement.

ACKNOWLEDGMENTS

This work is supported by the National Science Council and the Ministry of Education of Taiwan, ROC. We thank Prof. Ite Yu for lending us the wavelength meter.

-
- [1] C. S. Wood, S. C. Bennett, D. Cho, B. P. Masterson, J. Roberts, C. E. Tanner, and C. E. Wieman, *Science* **275**, 1759 (1997).
- [2] V. A. Dzuba, V. V. Flambaum, and J. S. M. Ginges, *Phys. Rev. D* **66**, 076013 (2002).
- [3] P. A. Vetter, D. M. Meekhof, P. K. Majumder, S. K. Lamoreaux, and E. N. Fortson, *Phys. Rev. Lett.* **74**, 2658 (1995).
- [4] N. H. Edwards, S. J. Phipp, P. E. G. Baird, and S. Nakayama, *Phys. Rev. Lett.* **74**, 2654 (1995).
- [5] B. C. Regan, E. D. Commins, C. J. Schmidt, and D. DeMille, *Phys. Rev. Lett.* **88**, 071805 (2002).
- [6] J. J. Hudson, D. M. Kara, I. J. Smallman, B. E. Sauer, M. R. Tarbutt, and E. A. Hinds, *Nature (London)* **473**, 493 (2011).
- [7] I. Fan, T.-L. Chen, Y.-S. Liu, Y.-H. Lien, J.-T. Shy, and Y.-W. Liu, *Phys. Rev. A* **84**, 042504 (2011).
- [8] B. Klöter, C. Weber, D. Haubrich, D. Meschede, and H. Metcalf, *Phys. Rev. A* **77**, 033402 (2008).
- [9] N.-C. Shie, W.-F. Hsieh, and J.-T. Shy, *Opt. Express* **19**, 21109 (2011).
- [10] A. D. Cronin, R. B. Warrington, S. K. Lamoreaux, and E. N. Fortson, *Phys. Rev. Lett.* **80**, 3719 (1998).
- [11] A. Lurio and A. G. Prodel, *Phys. Rev.* **101**, 79 (1956).
- [12] G. Gould, *Phys. Rev.* **101**, 1828 (1956).
- [13] T.-L. Chen, I. Fan, H.-C. Chen, C.-Y. Lin, S.-E. Chen, J.-T. Shy, and Y.-W. Liu, *Phys. Rev. A* **86**, 052524 (2012).
- [14] G. Hermann, G. Lasnitschka, and D. Spengler, *Z. Phys. D* **28**, 127 (1993).
- [15] N. Taylor, N. Omenetto, B. W. Smith, and J. D. Winefordner, *Appl. Phys. B* **89**, 99 (2007).
- [16] J.-T. Shy and T.-C. Yen, *Opt. Lett.* **12**, 325 (1987).
- [17] P. V. K. Kumar and M. V. Suryanarayana, *Opt. Commun.* **285**, 1838 (2012).
- [18] P. V. Kiran Kumar, M. Sankari, and M. V. Suryanarayana, *Phys. Rev. A* **87**, 012503 (2013).
- [19] “HighFinesse product manual”, <http://www.highfinesse.com/>.
- [20] T. J. Quinn, *Metrologia* **40**, 103 (2003).
- [21] R. Felder, *Metrologia* **42**, 323 (2005).
- [22] N.-C. Shie, S.-E. Chen, C.-Y. Chang, W.-F. Hsieh, and J.-T. Shy, *J. Opt. Soc. Am. B* **30**, 2022 (2013).
- [23] M. Nakazawa, *J. Appl. Phys.* **59**, 2297 (1986).
- [24] R. L. Kurucz, “Atomic spectral line database”, <http://cfa-www.harvard.edu/amp/ampdata/kurucz23/sekur.html>.
- [25] M. G. Kozlov, S. G. Porsev, and W. R. Johnson, *Phys. Rev. A* **64**, 052107 (2001).
- [26] R. S. Qydata, R. Bobkowski, E. Lisicki, and J. Szudy, *Z. Naturforsch. A* **42**, 559 (1987).